Phases of a phenomenological model of twisted bilayer graphene

J. F. Dodaro,[1] S. A. Kivelson,[1] Y. Schattner,[1,2] X. Q. Sun,[1] and C. Wang[1]

[1]*Department of Physics, Stanford University, Stanford, California 94305, USA*

[2]*Stanford Institute for Materials and Energy Sciences, SLAC National Accelerator Laboratory and Stanford University,*
Menlo Park, California 94025, USA

We propose a lattice-scale two-band generalized Hubbard model as a caricature of the electronic structure of twisted bilayer graphene. Various possible broken-symmetry phases can arise, including a nematic phase (which is a form of orbital ferromagnet) and an orbital-triplet spin-singlet superconducting phase. Concerning the mechanism of superconductivity, we propose an analogy with superconductivity in alkali-doped C_{60} in which a violation of Hund's first rule plays a central role.

I. INTRODUCTION

Twisted bilayer graphene makes a moiré pattern which defines an approximate triangular lattice with a large unit cell. Various band-structure calculations show that for certain twist angles, there are remarkably weakly dispersing bands near the Fermi surface [1,2]. In particular, the bands immediately above and below the charge neutrality point are thought to be approximately doubly degenerate; experiments [3,4] show that when one of these bands is filled with four holes per unit cell, $\bar{n}_h = 4$ ($\bar{n}_h$ denotes the number of holes per unit cell, relative to charge neutrality), there is behavior suggestive of a band insulator, while for the half-filled band, $\bar{n}_h = 2$, there is what appears to be an emergent insulating state at low temperatures ($T < 4$ K), possibly with broken symmetry. (Similar behavior occurs when electrons are added into these bands, $\bar{n}_h < 0$ in our convention.) As a function of $\bar{n}_h$, there is a pronounced peak in the resistivity at the charge neutrality point, $\bar{n}_h = 0$, where the resistivity is a mildly increasing function of decreasing T but does not show any clear tendency to diverge. For hole concentrations, $0 < \bar{n}_h < 2$ and $2 < \bar{n}_h < 4$, two superconducting domes with a maximal $T_c \approx 1.7$ K appear. (Superconductivity has not yet been detected for $\bar{n}_h < 0$.)

There are many complexities associated with the microscopic physics of this system; it may be impossible to define localized Wannier functions associated with the two bands just below the charge neutrality point without also including the two above the neutrality point [5,6]. Moreover, unless the twist angle is precisely commensurate, the system in question is in truth a quasicrystal, not a crystal at all. Nonetheless, to simplify the problem, we propose to study a two-orbital tight-binding model on the triangular lattice with predominantly on-site interactions, similar to the model introduced in Ref. [7], as a caricature of the physical problem. Note that by construction, our model is a band insulator at the charge neutrality point $\bar{n}_h = 0$, in apparent conflict with experiment, and it cannot describe fillings $\bar{n}_h < 0$. However, it is our hope that it is sufficient to shed light on the problem in a range of $\bar{n}_h$ near $\bar{n}_h \sim 2$.

In thinking about the interactions that enter the model, we should take into account the fact that these are effective interactions. In particular, since the typical graphene phonon has an energy $\hbar\omega_{\bar{q}} \sim 200$ meV [8,9], while the flat bands in twisted graphene are thought to have bandwidths of the order of 10 meV [3], the system is in an antiadiabatic limit in which it is reasonable to integrate out the phonons. This tends to lower the on-site repulsion between electrons and (from the "dynamical Jahn-Teller" effect) produce violations of Hund's rules. Even with purely repulsive microscopic interactions, correlation effects associated with integrating out high-energy electronic degrees of freedom can also lead to a reduction of the on-site repulsion and a violation of Hund's rule, as has been shown [10] for the $t - J$ model on a truncated icosahedron (C_{60}).

With these considerations in mind, a number of broken-symmetry phases are possible. From a weak-coupling perspective, the lack of any Fermi surface nesting on the triangular lattice reduces the susceptibility to translation symmetry breaking. From a complementary strong-coupling perspective, the triangular lattice is geometrically frustrated. We will thus focus on states that leave translation symmetry unbroken [11]. Specifically, we have found a regime in which there is an orbital ferromagnetic phase for a range of $\bar{n}_h$ that extends asymmetrically about $\bar{n}_h = 2$. Depending upon how we identify operators in the model with physical observables, the orbital ferromagnetism can be associated with various patterns of point-group symmetry breaking; for instance, it can represent nematic order. Moreover, the system can be insulating at $\bar{n}_h = 2$ if the order is sufficiently strong. Away from $\bar{n}_h = 2$ we find two superconducting domes with on-site, spin-singlet, orbital-triplet pairing.

II. A LATTICE-SCALE MODEL

We define a minimal lattice model with appropriate symmetries and the fewest degrees of freedom needed to account for the salient features summarized above. We consider a Hubbard-like model on a triangular lattice with a Wannier function

that transforms according to a two-dimensional irreducible representation of the point group. One could think of this as corresponding to d_{xy} and $d_{x^2-y^2}$ orbitals split from the other (filled or empty) d orbitals by crystal-field effects or, alternatively, as p_x and p_y orbitals. At a formal level, these two cases behave similarly, but their different symmetries have different implications for the nature of broken-symmetry phases. To be concrete, we will assume the d-orbital case.

We thus introduce a pseudospin index τ, such that $\tau = \pm 1$ corresponds to a $d \pm id$ combination of these orbitals. We neglect spin-orbit coupling, so there is an $SU(2)$ spin rotational symmetry, and reflecting an assumed conservation of pseudospin and time-reversal symmetry, there is an additional orbital $U(1) \times Z_2$ symmetry. Physically, this $U(1)$ symmetry is related to spatial rotations, and correspondingly, a more realistic band structure would include τ-dependent dispersion relations that would break the $U(1)$ symmetry to C_6; for the most part we will ignore this for simplicity. We thus consider the two-orbital model

$$H = H_0 + H_{int} + H'_{int} + H_{nn} \qquad (1)$$

in terms of creation operators $c^{\dagger}_{\vec{R},s,\tau}$ for electrons with spin and orbital polarizations s and τ on site $\vec{R}$. The band structure is given by the nearest-neighbor tight-binding model

$$H_0 = -t \sum_{\langle \vec{R}, \vec{R}' \rangle, s, \tau} [c^{\dagger}_{\vec{R},s,\tau} c_{\vec{R}',s,\tau} + \text{H.c.}]. \qquad (2)$$

The most general on-site interactions (consistent with the above-stated symmetries) can be expressed as a sum of the "important" interactions,

$$H_{int} = U \sum_{\vec{R}} [\hat{n}_{\vec{R}} - 2]^2 - K \sum_{\vec{R}} \left[\mathbf{L}_{\vec{R}} \cdot \mathbf{L}_{\vec{R}} - \delta L^z_{\vec{R}} L^z_{\vec{R}} \right], \quad (3)$$

where δ tunes between $X - Y$ and Ising-like characters, and additional interactions

$$H'_{int} = \sum_{\vec{R}} [U_3 + U_4(\hat{n}_{\vec{R}} - 2)](\hat{n}_{\vec{R}} - 1)(\hat{n}_{\vec{R}} - 2)(\hat{n}_{\vec{R}} - 3).$$

For simplicity, we ignore H'_{int}; that is, we set $U_3 = U_4 = 0$. H_{nn} is an additional further-neighbor interaction (assumed to be small) that we will introduce below. Here

$$\hat{n}_{\vec{R}} = \sum_{\tau,s} c^{\dagger}_{\vec{R},s,\tau} c_{\vec{R},s,\tau}, \qquad (4)$$

and the orbital pseudospin

$$\vec{L}_{\vec{R}} = \frac{1}{2} \sum_{\tau,\tau',s} c^{\dagger}_{\vec{R},s,\tau} \vec{\sigma}_{\tau,\tau'} c_{\vec{R},s,\tau'}. \qquad (5)$$

To better appreciate the significance of K, consider the single-site problem with two electrons: For $K > 0$, the spin-triplet states have higher energy than the singlet, in violation of Hund's first rule [12]. Indeed, in the following we will assume $K > 0$, which, as already indicated, involves the nontrivial effects of high-energy degrees of freedom that have been integrated out.

The assumption that further-neighbor interactions H_{nn} are relatively small deserves comment as well. Of course, Coulomb interactions are long range, but in the devices in question, there is a metallic gate separated from the bilayer by a distance comparable to the size of a unit cell in the moiré pattern. We invoke this as the justification for assuming that further-neighbor interactions are weak and can mostly be neglected. Since the bare interactions between electrons are strongly repulsive, it is likely that $U > 0$, although possibly, due to the effects of electron-phonon coupling and other correlation effects, it may be smaller than naive estimates suggest, and we will even consider the case in which it is less than K.

We also include in our model a (weak) nearest-neighbor interaction,

$$H_{nn} = -\widetilde{K} \sum_{\langle \vec{R}, \vec{R}' \rangle} \mathbf{L}_{\vec{R}} \cdot \mathbf{L}_{\vec{R}'}, \qquad (6)$$

and take $K \gg \widetilde{K} > 0$. The latter condition implies that H_{nn} favors orbital ferromagnetism, as would be expected for a direct exchange interaction. Because the triangular lattice is nonbipartite, the sign of t is significant. We will take $t < 0$ on a phenomenological basis to reproduce the observed sense of the particle-hole asymmetry about $\overline{n}_h = 2$ and will in some places consider the effects of more complex band structures, i.e., the effects of further-neighbor hopping.

III. MEAN-FIELD THEORY

For weak coupling, a reliable solution can be obtained using Hartree-Fock/BCS mean-field theory. In this limit, the only generic instability is to superconductivity. If we nevertheless apply the same approach for intermediate couplings, the results, while not well justified, are highly suggestive. Because we have dominantly on-site interactions, the only possible order parameters are on site. If we assume translation symmetry is unbroken, then these consist of orbital or spin ferromagnetism and superconductivity involving on-site pairing. Since we are assuming $K > 0$, spin ferromagnetism can be neglected, and of the possible superconducting channels, only orbital pseudospin-triplet spin-singlet pairing is favored. To simplify the equations, in this section we will take $\widetilde{K} = 0$.

To implement this approach, we define a trial Hamiltonian H_{tr} (henceforth summation over spin and pseudospin indices, s and τ, is implicit):

$$H_{tr} = \sum_k \epsilon_k c^{\dagger}_{k,s,\tau} c_{k,s,\tau} - \vec{h} \cdot \sum_{\vec{R}} \vec{L}_{\vec{R}}$$
$$+ \sum_{\vec{R}} \{ c^{\dagger}_{\vec{R},\uparrow,\tau} [(\vec{d} \cdot \vec{\sigma}) i\sigma_y]_{\tau,\tau'} c^{\dagger}_{\vec{R},\downarrow,\tau'} + \text{H.c.} \}, \qquad (7)$$

where $\vec{h}$, $\vec{d}$, and ϵ_k are variational parameters corresponding to orbital ferromagnetism, triplet superconductivity, and band structure, respectively. Under time-reversal Θ, $\vec{h}_{\parallel} \rightarrow \vec{h}_{\parallel}, h_z \rightarrow -h_z, \vec{d}_{\parallel} \rightarrow -\vec{d}_{\parallel}$, and $d_z \rightarrow d_z$, where $\vec{h}_{\parallel}$ and $\vec{d}_{\parallel}$ are the $X - Y$ components of $\vec{h}$ and $\vec{d}$, respectively. $F_{var} \equiv F_{tr} + \langle H - H_{tr} \rangle_{tr}$ is a variational upper bound to the free energy. The corresponding mean-field equations are

$$h_j = V^F_j \langle L_j(\vec{R}) \rangle, \qquad (8)$$

$$d_j = -V^{sc}_j \langle c_{\vec{R}\uparrow\tau} [\sigma_j(i\sigma_y)]^*_{\tau\tau'} c_{\vec{R}\downarrow\tau'} \rangle, \qquad (9)$$

where $V_x^F = V_y^F = 2U + \frac{K}{2}(5 - \delta)$, $V_z^F = 2U + \frac{K}{2}(5 - 3\delta)$, $V_x^{sc} = V_y^{sc} = U - \frac{K}{4}(1 - \delta)$, $V_z^{sc} = U - \frac{K}{4}(1 + \delta)$, and there is a shift in the chemical potential. For weak coupling, the superconducting T_c is determined by whichever component of V_j^{sc} is most attractive:

$$T_c \sim W e^{-1/2N_0|V_j^{sc}|}, \tag{10}$$

where N_0 is the density of states at the Fermi level and W is the bandwidth. If $\delta > 0$, then $\vec{d} = d\hat{z}$, and the superconducting state preserves time-reversal and $U(1) \times Z_2$ orbital symmetries. If $\delta < 0$, then $\vec{d}$ lies in the $X - Y$ plane and may give rise to a rich variety of superconducting phases whose symmetries will be discussed at the end of this section.

Orbital ferromagnetism is possible at stronger coupling when the interactions exceed an appropriate Stoner criterion. For $\delta > 0$, the orbital moment $\langle \vec{L} \rangle$ lies in the $X - Y$ plane and breaks the orbital $U(1)$ symmetry; this is a form of nematic order. For $\delta < 0$, $\langle \vec{L} \rangle = L\hat{z}$; time reversal symmetry is broken but the orbital $U(1)$ symmetry is preserved.

The full mean-field solution of Eqs. (8) and (9) was obtained numerically for the $\delta > 0$ case. Representative mean-field phase diagrams are shown in Fig. 1 for $U = 0$, $K = 4$, $t = -1$, and $\delta = 0.3$ and in Fig. 2 for $U = 0$, $K = 2$, $t = -1$, $\delta = 0.3$, and including a second-neighbor hopping, $t' = -0.4$. The solid lines represent continuous phase boundaries, while the double lines mark discontinuous transitions. The broken symmetries are as indicated, where 2P signifies a forbidden region of density in which two-phase coexistence occurs and SC and NSC refer, respectively, to superconducting and nematic superconducting phases.

The NSC exhibits a mixture of the pairing symmetries discussed above: the predominant channel has $d_z \neq 0$; however, the nematic order induces a nonzero $X - Y$ component of $\vec{d}$. Moreover, the $X - Y$ components of $\vec{d}$ are related to the nematic order parameter $\vec{h}$: for $h_x \neq 0$, the NSC state has real d_z, imaginary d_y, and $d_x = 0$. The NSC therefore breaks gauge invariance and time reversal simultaneously. The pattern of order in the NSC phase can be understood by considering the symmetry-allowed cubic terms that couple $\vec{h}$ and $\vec{d}$ in the Landau free energy $\mathcal{F}$,

$$\mathcal{F}(T) = \cdots + ia_1(T)\vec{h}_\parallel \cdot (\vec{d}^* \times \vec{d})_\parallel + ia_2(T)h_z(\vec{d}^* \times \vec{d})_z, \tag{11}$$

where $a_i(T)$ are temperature-dependent coefficients. Outside the nematic phase, the SC state has pure $d_z \neq 0$ order.

For the $K = 4$ case shown in Fig. 1, the orbital pseudospin is fully polarized in the ground state for a range of $\bar{n}_h$ (indicated by the thick black line) bounded from above by a mild quantum critical point at $\bar{n}_h = n_{c1} = 3.5$ (marked by the cross) and from below by a first-order point at $\bar{n}_h = n_{c2} \approx 1.9$. The system is insulating at $\bar{n}_h = 2$. If we were to suppress superconductivity (say, by application of a magnetic field), then we would find a (nematic) half-metallic orbital ferromagnet in this range of $\bar{n}_h$ (as long as $\bar{n}_h \neq 2$), and the transition that occurs at $\bar{n}_h = n_{c1}$ would be a Lifshitz transition.

For the $K = 2$ case shown in Fig. 2, while there is a broad nematic phase, the order is not sufficiently strong to produce insulating behavior at $\bar{n}_h = 2$. Moreover, here we find that
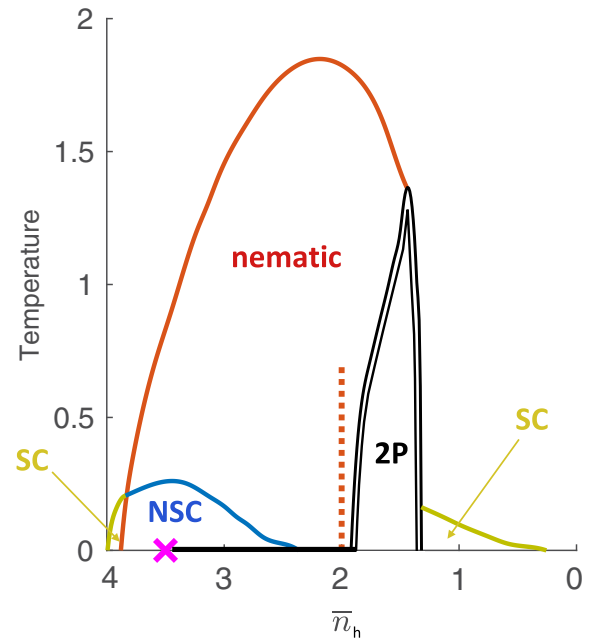

FIG. 1. Mean-field phase diagram with parameters $U = 0$, $K = 4$, $t = -1$, $\delta = 0.3$, and $\widetilde{K} = 0$ (temperature is measured in units of $|t|$). Note that the number of electrons per unit cell in the band immediately below charge neutrality $\bar{n}_e$ is given by $4 - \bar{n}_h$. Various broken-symmetry phases are indicated in the diagram, where SC and NSC are, respectively, a superconducting phase with only $d_z \neq 0$ and a nematic superconducting phase in which, in addition, the in-plane component of $\vec{d}$ perpendicular to $\vec{h}$ is nonzero. The orbital ferromagnetic phase with $h_x \neq 0$ is fully polarized at $T = 0$ for $n_{c1} \geqslant \bar{n}_h \geqslant n_{c2}$, as indicated by the solid black line. This further implies that the ground state at $\bar{n}_h = 2$ is insulating. The dashed line at $\bar{n}_h = 2$ has a height corresponding to the insulating gap $|h_x| - W \approx 0.7$, where W is the bandwidth. The regime labeled 2P is a forbidden regime, where two phases coexist macroscopically. Solid colored lines represent continuous transitions, and double lines indicate discontinuous ones. The cross at $\bar{n}_h = n_{c1}$ is a quantum critical point.

all the transitions appear to be continuous. For substantially smaller K, there is no nematic phase at all.

If we were to include fluctuations beyond the mean-field treatment, since the nematic phase breaks $U(1)$ symmetry, the ordered phase at finite temperature would presumably be replaced by a power-law phase. If crystal-field effects were included that reduce $U(1)$ to C_6, there could be a sequence of two transitions involving an ordered phase and a power-law phase. Clearly, all superconducting phases at nonzero T would be replaced by phases with quasi-long-range order.

We now turn to address the possible phases for $\delta < 0$. As mentioned above, we expect an orbital ferromagnetic phase with $h_z \neq 0$, which breaks time-reversal symmetry but preserves the orbital rotational symmetry. From Eq. (9), the leading superconducting instability leads to a nonzero $\vec{d}_\parallel$. The two-component nature of the order parameter can, by analogy to the case of Sr$_2$RuO$_4$ [13], lead to a number of different superconducting states. For simplicity, here we focus on states which can be reached from the nonsuperconducting phases by a continuous transition, i.e., those that break the minimal number of additional symmetries. Importantly, inside
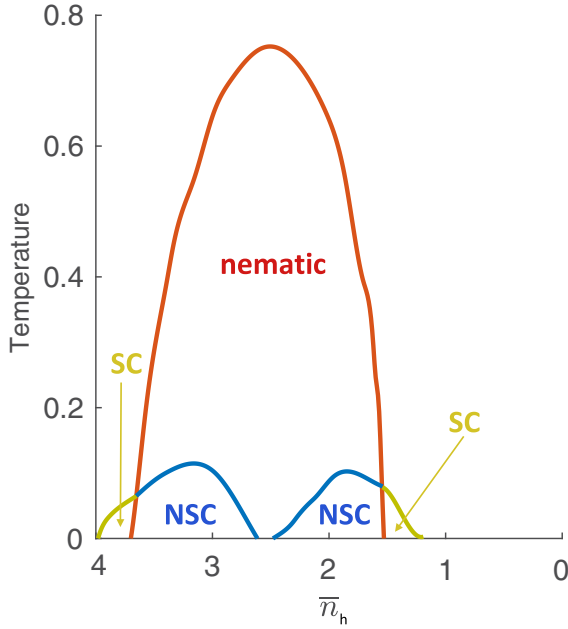
FIG. 2. Mean-field phase diagram with parameters $U = 0$, $K = 2$, $t = -1$, $\delta = 0.3$, and $\widetilde{K} = 0$ and with a second-neighbor hopping $t' = -0.4$. Symbols are as in Fig. 1. The state at $\overline{n}_h = 2$ is conducting, and all transitions appear to be continuous.

the orbital ferromagnetic dome, Eq. (11) implies the relative phases of the d_x and d_y components lock in a way that preserves the orbital rotational symmetry. The different phases and corresponding broken symmetries that follow from Eq. (11) are shown in Table I for both signs of δ.

IV. STRONG-COUPLING LIMIT

In much the same way as the $t - J$ model can be derived as the strong-coupling limit of the Hubbard model, we can derive an effective model that captures the low-energy physics of our two-band Hubbard model in the strong-coupling limit where t is small compared to the on-site interactions. Here we map the problem to a lattice gas of hard-core particles. Let $\overline{n}_e$ be the number of electrons per unit cell in the band immediately below charge neutrality, $\overline{n}_e = 4 - \overline{n}_h$. For compactness we consider the case in which δ is small. We further restrict our attention to $U > -K/2$ and the range $0 \leqslant \overline{n}_e \leqslant 2$, but the case

TABLE I. Broken (in square brackets) and unbroken symmetries for the normal ($\vec{h} \neq 0$) state and various superconducting phases for $\delta < 0$ (Ising-like) and $\delta > 0$ ($X - Y$-like). The two choices of irreducible representations for the orbitals, $p \pm ip$ and $d \pm id$, are identical under rotation and time-reversal symmetries. However, mirror symmetries are affected differently in the two cases, and they also depend on which mirror plane one is considering.

	X-Y-like	Ising-like
Normal ($\vec{h} \neq 0$)	$[C_6]$, Θ, C_2	$[\Theta]$, C_6
SC ($\vec{h} \neq 0$)	$[C_6, \Theta]$, C_2	$[\Theta]$, C_6
SC ($\vec{h} = 0$)	C_6, Θ	$[\Theta]$, C_6

$2 \leqslant \overline{n}_e \leqslant 4$ can be obtained from these results by a straightforward particle-hole transformation, which involves taking $t \to -t$. For $U > -K/2$, two doubly occupied sites have lower energy than either one singly and one triply occupied sites or one quadruply occupied site and one empty site. Given this, for $0 \leqslant \overline{n}_e \leqslant 2$, we can project out the triply and quadruply occupied states. Now

$$H_{\text{int}} = \sum_{\vec{R}} [\varepsilon_b b^\dagger_{\vec{R},m} b_{\vec{R},m} + \varepsilon_a a^\dagger_{\vec{R},\tau,s} a_{\vec{R},\tau,s} + 4U \hat{v}_{\vec{R}}], \quad (12)$$

where $\varepsilon_b \equiv -2K$, $\varepsilon_a \equiv U - 3K/4$, and there is a hard-core constraint that $\hat{v}_{\vec{R}} \geqslant 0$ for all $\vec{R}$, where $\hat{v}_{\vec{R}}$ is the density of empty sites,

$$\hat{v}_{\vec{R}} = 1 - b^\dagger_{\vec{R},m} b_{\vec{R},m} - a^\dagger_{\vec{R},\tau,s} a_{\vec{R},\tau,s}, \quad (13)$$

and the electron density is $2 - \hat{v}_{\vec{R}}$. Here we represent doubly occupied sites as being occupied by a spinless $L = 1$ boson with $L_z = m = -1, 0, 1$, with creation operator $b^\dagger_{\vec{R},m}$, while singly occupied sites are represented by $S = 1/2$, $L = 1/2$ fermions, with creation operator $a^\dagger_{\vec{R},\tau,s}$.

It is then easy to see that for $\overline{n}_e = 2$ there is a Mott insulating state with one boson per site. For $U > K/4$, in the range $1 < \overline{n}_e < 2$, the system is a mixture of $\langle a^\dagger_{\vec{R},\tau,s} a_{\vec{R},\tau,s} \rangle = (2 - \overline{n}_e)$ fermions and $\langle b^\dagger_{\vec{R},m} b_{\vec{R},m} \rangle = \overline{n}_e - 1$ bosons, while for $0 < \overline{n}_e < 1$, it contains a concentration $\langle a^\dagger_{\vec{R},\tau,s} a_{\vec{R},\tau,s} \rangle = \overline{n}_e$ fermions and no bosons. On the other hand, for $K/4 > U > -K/2$, in the entire range $0 < \overline{n}_e < 2$ the system consists purely of bosons with $\langle b^\dagger_{\vec{R},m} b_{\vec{R},m} \rangle = \overline{n}_e/2$.

We now consider the effect of the additional terms in the Hamiltonian. In the obvious way, H_{nn} can be rewritten as a nearest-neighbor orbital pseudospin-dependent interaction between the bosons and fermions. To first order in t two terms are generated: a hopping term for fermions between nearest-neighbor sites $\vec{R}$ and $\vec{R}'$,

$$-t[a^\dagger_{\vec{R},\tau,s} a_{\vec{R}',\tau,s} + \text{H.c.}], \quad (14)$$

and a nearest-neighbor boson-fermion interchange,

$$t/2[(b^\dagger_{\vec{R},m} \vec{T}_{m,m'} b_{\vec{R}',m'}) \cdot (a^\dagger_{\vec{R}',\tau,s} \vec{\sigma}_{\tau,\tau'} a_{\vec{R},\tau',s}) + \text{H.c.}]$$
$$+ t/2[b^\dagger_{\vec{R},m} b_{\vec{R}',m} a^\dagger_{\vec{R}',\tau,s} a_{\vec{R},\tau,s} + \text{H.c.}], \quad (15)$$

where $\vec{T}$ is the pseudo-spin-1 generators of rotations.

Finally, there are a variety of terms that are generated in higher-order perturbation theory in powers of t, which are thus assumed to be small compared to terms of order t. Of these, the two most important are a renormalization of the interaction in H_{nn} acting between two neighboring sites occupied by bosons,

$$\widetilde{K} \to \widetilde{K}^{\text{eff}} = \widetilde{K} - \frac{4t^2}{4U + 5K}, \quad (16)$$

and a nearest-neighbor hopping term for the bosons with matrix element

$$t^{\text{eff}} = \frac{t^2}{K - 4U}. \quad (17)$$

The first term is potentially important in the state at $\overline{n}_e = 2$; here the symmetry of the Mott insulator changes from orbital

ferromagnetism for $\widetilde{K}^{\text{eff}} > 0$ to orbital antiferromagnetism for $\widetilde{K}^{\text{eff}} < 0$. The boson hopping term is small compared to the boson-fermion exchange, and so it is important only when there are no fermions to induce delocalization of the bosons, i.e., when $K/4 > U > -K/2$. Note that there is an interesting breakdown of perturbation theory near the upper end of this regime.

The physics of the resulting lattice gases is itself rich and interesting. The case of orbital pseudospin-1 bosons (relevant for $K/4 > U > -K/2$) is similar to the problem of spin-1 bosons that has been studied in the context of cold atomic gases [14]. For ferromagnetic $\widetilde{K} > 0$, this results in the existence of a spin-polarized Bose condensate [15,16], while for antiferromagnetic $\widetilde{K} < 0$, there are multiple possible states, including fractured condensates [17]. The more interesting case in which there is a boson-fermion mixture ($U > K/4$ and $1 < \overline{n}_e < 2$) has an analog in the problem of ^{3}He-^{4}He mixtures [18]. Various forms of superfluid states as well as phase-separated states are possible depending on the parameters.

One feature of the strong-coupling limit ($U \to \infty$) that is particularly striking is a strong asymmetry in the orbital ferromagnetism between $\overline{n}_e < 2$ and $\overline{n}_e > 2$. This can be seen by studying the analog of the Nagaoka problem [19]: either one doped electron or one doped hole relative to $\overline{n}_e = 2$. For $t < 0$, Nagaoka's theorem applies to one hole but not to one electron. More detailed analysis [20,21] shows that dilute concentrations of doped holes make an effective ferromagnetic contribution to $\widetilde{K}^{\text{eff}}$ proportional to $t(2 - \overline{n}_e)$, while doped electrons make a corresponding antiferromagnetic contribution. While this result is restricted to infinite U and vanishing doping density, in the next section we will show that the basic physics is much more robust [22].

V. EXACT DIAGONALIZATION

We have studied the model in Eq. (1) on the $N = 4$ site cluster shown in Fig. 3 for various values of U. We have taken units such that $t = -1$ and have arbitrarily taken $K = 2$, $\widetilde{K} = 0.2$, and $\delta = 0$. [This latter condition implies an enlarged $SU(2)$ orbital symmetry, and therefore L is conserved.] This is a small system, but it is large enough to allow us to make crude estimates of interesting properties of the system at intermediate coupling, where analytic approaches fail. The results with various numbers of electrons are representative
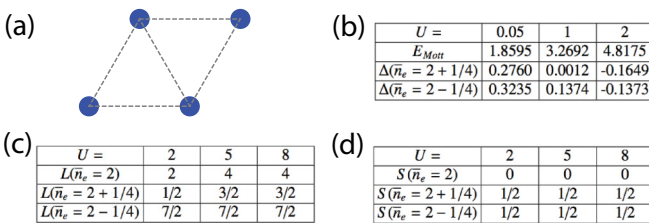
of the properties of a larger system with values of $\overline{n}_e = 2$, $2 \pm 1/4$, $2 \pm 1/2$, etc. We compute the total orbital pseudospin L; if this takes its maximal allowed value, $L(\overline{n}_e) = L_{\max}(\overline{n}_e) = N\overline{n}_e/2$, then this suggests that the larger system will exhibit a fully polarized orbital ordered state, while there is likely no orbital ferromagnetism in the thermodynamic limit if L takes its minimal value $L(\overline{n}_e) = L_{\min}(\overline{n}_e)$, where $L_{\min}(\overline{n}_e) = 0$ or $1/2$ depending on whether $N\overline{n}_e$ is even or odd. From the ground-state energy as a function of electron number $E(N_{el})$, we define two particularly interesting "gaps,"

$$E_{\text{Mott}} \equiv E(2N + 1) + E(2N - 1) - 2E(2N) \quad (18)$$

and, for $\overline{n}_e \neq 1$, 2, or 3 and under conditions $N\overline{n}_e = $ odd,

$$\Delta(\overline{n}_e) \equiv [2E(\overline{n}_e N) - E(\overline{n}_e N + 1) - E(\overline{n}_e N - 1)]/2. \quad (19)$$

These quantities are defined such that, if there were an insulating state at $\overline{n}_e = 2$, then E_{Mott} would indeed approach the Mott gap in the limit $N \to \infty$ and, if the doped system were to have a nodeless superconducting gap, then $\Delta(\overline{n}_e)$ would approach the value of the minimal gap in the same limit. Some results for $L(\overline{n}_e)$, $S(\overline{n}_e)$, E_{Mott}, and $\Delta(\overline{n}_e)$ are reported in Fig. 3. In the case $\overline{n}_e < 2$, the system is a fully polarized orbital ferromagnet, while in the case $\overline{n}_e > 2$, the orbital pseudospin is far from being fully polarized. There is a superconducting gap $\Delta(\overline{n}_e) > 0$ when U is small that is destroyed for larger U.

VI. EXACT RESULTS FOR $U = K/4$

Under the special condition $U = K/4$ with $\delta = 0$ and $\widetilde{K} = 0$, the model defined in Eq. (1) becomes effectively noninteracting in the sector of Hilbert space with maximal orbital pseudospin [23]. The model itself is still strongly interacting; it is just in this sector that the interactions effectively vanish. It still depends on $\overline{n}_e$ and U whether or not the ground state is a fully polarized orbital ferromagnet. When this is the case, if $\overline{n}_e = 2$, the system is insulating, while for $\overline{n}_e \neq 2$ it forms a half-metallic orbital ferromagnetic Fermi gas.

It is also interesting to consider what happens upon perturbing about this solvable line. For small $\widetilde{K} > 0$ or $U < K/4$, there are effective weak attractive interactions induced between like-orbital pseudospin electrons, and this in turn leads, via the usual BCS mean-field analysis, to a spin-singlet orbital pseudospin-triplet superconducting state of the sort discussed in the mean-field analysis above. Otherwise, the effective interactions are repulsive, and any superconducting state that arises will have unconventional pairing and will arise by a version of the Kohn-Luttinger mechanism or through the exchange of a collective boson leading to a parametrically lower T_c.

VII. RELATION TO OTHER WORK

Not surprisingly, the discovery of superconductivity in twisted bilayer graphene has produced a flurry of "rapid-response" theories [6,24–29], of which the present paper is one. It is important to stress that the experimental situation is still evolving, so the applicability of any theoretical proposal is presently difficult to judge.

Our perspective differs from that of the other papers of which we are aware in several important ways. Many of these

(b)

$U =$	0.05	1	2
E_{Mott}	1.8595	3.2692	4.8175
$\Delta(\overline{n}_e = 2 + 1/4)$	0.2760	0.0012	-0.1649
$\Delta(\overline{n}_e = 2 - 1/4)$	0.3235	0.1374	-0.1373

(c)

$U =$	2	5	8
$L(\overline{n}_e = 2)$	2	4	4
$L(\overline{n}_e = 2 + 1/4)$	1/2	3/2	3/2
$L(\overline{n}_e = 2 - 1/4)$	7/2	7/2	7/2

(d)

$U =$	2	5	8
$S(\overline{n}_e = 2)$	0	0	0
$S(\overline{n}_e = 2 + 1/4)$	1/2	1/2	1/2
$S(\overline{n}_e = 2 - 1/4)$	1/2	1/2	1/2

FIG. 3. (a) The four-site system that we treat by exact diagonalization using the Hamiltonian in Eq. (1). We take $K = 2$, $t = -1$, $\delta = 0$, $\widetilde{K} = 0.2$, and various values of U. (b) The quantities E_{Mott} and $\Delta(\overline{n}_e)$ are defined in Eqs. (18) and (19). (c) The total orbital pseudospin of the ground state for various $\overline{n}_e$. (d) The total spin of the ground state for various $\overline{n}_e$.

works make an implicit analogy with the cuprates in identifying the insulating behavior at $\overline{n}_h = 2$ as "Mott insulating" and looking for possible mechanisms of unconventional pairing in which the pair-wave function vanishes for two electrons on the same site. These papers all envisage the dominant interaction to be a strongly repulsive Hubbard U, and where weaker interactions are considered, they are ones that, for example, favor Hund's rule states with maximal spin. In contrast, we have explored the possibility that a combination of correlation effects (involving bands that have been integrated out) and electron-phonon effects leads to a reduction of U and violations of Hund's rule, analogous to the situation that is believed to apply in alkali-doped C_{60}. We have proposed a large role for orbital pseudospin ferromagnetic ordering, including identifying this broken symmetry as the cause of the insulating phase. Moreover, we have suggested that the large asymmetry in the behavior of the quantum oscillations for $4 > \overline{n}_h > 2$ versus $2 > \overline{n}_h > 0$ is associated with Nagaoka-type stabilization of the orbital ferromagnetism for one sign of doping but not the other. We have also found a superconducting state that is largely conventional with on-site spin-singlet pairing (albeit with possibly interesting orbital pseudospin structure).

There are also some important differences and similarities in the models considered. The model we study is in large part the same as that introduced in Ref. [7], although they considered it in a very different range of parameters (where, for example, Hund's first rule is obeyed). As mentioned earlier, several papers [5,6] have noted that there are significant theoretical barriers to a direct route from the nodal band structure of the individual graphene sheets to the effective two-orbital model we have studied. We have no disagreement with this conclusion; we view our model as a phenomenological construct.

An ambitious approach to connecting the microscopics to the observed phenomena is reported in Ref. [5]. In contrast to our paper, this discussion purports to deal with the strong repulsive interactions between the conduction electrons without invoking the high-energy renormalizations discussed above. On the other hand, from a correspondingly more complex analysis, they also identify the Mott insulating phase as being the same sort of nematic as we have found and have suggested that the superconducting state has a spin-singlet s-wave gap structure. The principal mechanism of pairing in their work is the exchange of collective fluctuations; we, too, think this could play a role [30], but since we already obtain pairing at the mean-field level, we imagine that the main role of such fluctuations is to enhance T_c in the neighborhood of the nematic quantum critical point [31,32].

VIII. RELATION TO EXPERIMENT IN TWISTED BILAYER GRAPHENE

We have introduced a two-band Hubbard-like model on a triangular lattice as the simplest lattice-scale model with enough degrees of freedom to account for certain salient features of present experimental observations [3,4] in twisted bilayer graphene, doped with a concentration $\overline{n}$ of holes relative to charge neutrality. Even this stripped-down model is complex and has a large variety of possible ordered phases and phase diagram topologies as a function of the various interactions, some of which we have elucidated. In this final section, we

summarize some of these results and their possible relevance to bilayer graphene.

In the strong-coupling limit, we find a Mott insulating state at $\overline{n}_h = 2$ in the sense that the insulating behavior begins at a high temperature and exhibits a gap associated directly with the on-site interactions. The scale of this gap is large compared to intersite couplings and hence to the temperatures at which any ordering phenomena occur. This behavior is analogous to what is seen in the cuprates, where the gap in the insulating state of the undoped parent compounds is of the order of 2 eV, while all ordering phenomena occur at around room temperature or below. Such behavior is *not* seen in twisted bilayer graphene, where the resistivity changes from a high-temperature metallic behavior to a low-temperature insulating behavior at 4 K, which is just over a factor of 2 larger than the largest superconducting T_c. We thus conclude that it is likely that the insulating behavior in bilayer graphene is associated with a broken-symmetry state and should be associated with the intermediate-coupling regime of parameters in our model.

One attractive candidate for the insulating state is a fully polarized orbital ferromagnet. Depending on the sign of δ, this state can have either $X - Y$ character, in which case it is some sort of electron nematic state, or Ising character, in which case it breaks time-reversal symmetry and would result in a zero-field anomalous Hall effect and an offset in the quantum oscillations in the metallic state away from $n_h = 2$. While a fully polarized nematic state occurs naturally in the strong-coupling limit, it is unclear down to what level of couplings it survives. Nonetheless, we do find such an insulating state in our mean-field treatment at intermediate values of $K \sim E_F$ (see Fig. 1).

One interesting feature of the nematic state that arises naturally in the strong-coupling limit is an intrinsic particle-hole asymmetry with respect to doping away from $\overline{n}_h = 2$. Doping to $\overline{n}_h > 2$ produces an additional tendency to orbital ferromagnetism (induces an effective increase in the magnitude of $\widetilde{K}$), while $\overline{n}_h < 2$ favors orbital antiferromagnetism (tends to make $\widetilde{K}$ negative). Needless to say, orbital ferromagnetism is entirely unfrustrated even on a triangular lattice, while orbital antiferromagnetism is highly frustrated and likely has a much reduced ordering temperature, if it orders at all. The same particle-hole asymmetry around $\overline{n}_h = 2$ appears as a robust feature in the exact diagonalization analysis for intermediate couplings and can occur at mean-field level as well, provided the density of states is sufficiently asymmetric, as can be seen in Figs. 1 and 2.

For $\overline{n}_h > 2$, if we assume that the system is a fully polarized orbital ferromagnetic Fermi liquid, then from Luttinger's theorem it follows that the area enclosed by the Fermi surface is $A = A_0(\overline{n}_h - 2)/2 \mod A_0$, where A_0 is the area of the Brillouin zone. By contrast, if for a range of $\overline{n}_h < 2$ the system forms an unpolarized Fermi liquid, then the area enclosed by the Fermi surface is $A = A_0 n_h/4$. These expressions are loosely consistent with what has been inferred from quantum oscillation experiments in twisted bilayer graphene.

The conjectured nematicity, if it exists in the ground state, would necessarily begin at a finite transition temperature $T_F(\overline{n}_h)$. In a homogeneous system, this would imply the existence of singular temperature dependences of various measured quantities. No such singular behavior has been

observed. However, there are reasons to believe that the electronic structure of currently available materials is somewhat inhomogeneous, which would lead to a rounding of such singularities. We would thus tentatively like to associate the temperature of the observed metal-insulator crossover with this phase transition. This temperature appears to be maximal around $\overline{n}_h = 2$ and to drop smoothly with increasing $\overline{n}_h$, extrapolating to zero at a critical doping $\overline{n}_{h,c} \approx 2.4$. In this interpretation, n_c is associated with a nematic quantum critical point. The fact that this critical point roughly coincides with the hole doping at which the maximal T_c occurs invites analogy with the phase diagrams of the Fe-based high-temperature superconductors, where nematic quantum critical fluctuations have been conjectured to enhance T_c [31–33].

Turning now to the primary mechanism of superconductivity, the same interactions that promote the nematic order also give rise to superconductivity. We find spin-0 pseudospin-1 pairing with a substantial on-site component. In this sense, the superconducting state reflects the existence of attractive interactions. We suggest that a good analogy exists with another C-based superconductor, alkali-doped C_{60}, where effective intramolecular attractive interactions are generated by a (still somewhat unresolved) combination of intramolecular strong-correlation effects [10,34] and electron-phonon couplings [35–42]. In the calculations we have performed, this physics is encoded in the assumed values of U (assumed to be relatively small) and K (assumed to be positive). This is in contrast to the situation in unconventional superconductors where the interactions are strongly repulsive, and significant (albeit often very short range correlated) antiferromagnetic correlations often coexist with superconductivity.

The spin-singlet character of the superconducting order is consistent with the relatively small value of the in-plane critical field observed in experiment. At least the form of the pair wave function should be clarified once some spectroscopic probes of the gap structure, possibly tunneling experiments, are carried out. Somewhat in analogy with the situation in ^{3}He, there is a complex order parameter space associated with the pseudo-spin-1 character of the pairing which can lead to interesting textures and topology. A tendency to phase separation of the sort shown in Fig. 1 could lead to an enhanced susceptibility to the formation of electronically inhomogeneous states, even in otherwise relatively homogeneous samples.

[1] J. M. B. Lopes dos Santos, N. M. R. Peres, and A. H. Castro Neto, Phys. Rev. Lett. **99**, 256802 (2007).

[2] R. Bistritzer and A. H. MacDonald, Proc. Natl. Acad. Sci. USA **108**, 12233 (2011).

[3] Y. Cao, V. Fatemi, A. Demir, S. Fang, S. L. Tomarken, J. Y. Luo, J. D. Sanchez-Yamagishi, K. Watanabe, T. Taniguchi, E. Kaxiras, R. C. Ashoori, and P. Jarillo-Herrero, Nature (London) **556**, 80 (2018).

[4] Y. Cao, V. Fatemi, S. Fang, K. Watanabe, T. Taniguchi, E. Kaxiras, and P. Jarillo-Herrero, Nature (London) **556**, 43 (2018).

[5] H. C. Po, L. Zou, A. Vishwanath, and T. Senthil, arXiv:1803.09742.

[6] N. F. Q. Yuan and L. Fu, Phys. Rev. B **98**, 045103 (2018).

[7] C. Xu and L. Balents, arXiv:1803.08057 (2018) [Phys. Rev. Lett. (to be published)].

[8] A. C. Ferrari, J. C. Meyer, V. Scardaci, C. Casiraghi, M. Lazzeri, F. Mauri, S. Piscanec, D. Jiang, K. S. Novoselov, S. Roth, and A. K. Geim, Phys. Rev. Lett. **97**, 187401 (2006).

[9] T. Ando, J. Phys. Soc. Jpn. **76**, 104711 (2007).

[10] H. C. Jiang and S. A. Kivelson, Phys. Rev. B **93**, 165406 (2016).

[11] While these considerations are valid on the triangular lattice, translation symmetry breaking is very natural on a hexagonal lattice and should also be considered when making a comparison with the physical system.

[12] We have not included an explicit $J \vec{S} \cdot \vec{S}$ coupling because this can be absorbed as a shift of U and K.

[13] M. Sigrist, D. Agterberg, A. Furusaki, C. Honerkamp, K. K. Ng, T. M. Rice, and M. E. Zhitomirsky, Phys. C (Amsterdam, Neth.) **317**, 134 (1999).

[14] F. Zhou, Int. J. Mod. Phys. **17**, 2643 (2003).

[15] T. L. Ho, Phys. Rev. Lett. **81**, 742 (1998).

[16] T. Ohmi and K. Machida, J. Phys. Soc. Jpn. **67**, 1822 (1998).

[17] T. L. Ho and S. K. Yip, Phys. Rev. Lett. **84**, 4031 (2000).

[18] M. Blume, V. J. Emery, and R. B. Griffiths, Phys. Rev. A **4**, 1071 (1971).

[19] Y. Nagaoka, Phys. Rev. **147**, 392 (1966).

[20] C. N. Sposetti, B. Bravo, A. E. Trumper, C. J. Gazza, and L. O. Manuel, Phys. Rev. Lett. **112**, 187204 (2014).

[21] We have shown by an explicit variational calculation that in the $U \to \infty$ limit of the present model, the ground state of a finite-size system with one doped hole is a fully polarized orbital ferromagnet, consistent with Nagaoka's theorem, while for one doped electron an antiferromagnetic state has lower energy.

[22] If U is sufficiently large, it is possible to find insulating states at $n_h = 1$ and $n_h = 3$, which is clear from the strong-coupling analysis. In this limit, each site has a spin $1/2$ and an orbital spin $1/2$, the ordering of which is described by some sort of effective model. If we continue to stick to states that do not break translation symmetry, then the states in question will exhibit both orbital and spin ferromagnetism. Consequently, nearby metallic phases would be nematic if the orbital ferromagnetism has $X - Y$ character and would exhibit an anomalous Hall effect in the Ising case. This is, however, a very different parameter range, reflecting very different microscopic physics, than we have considered in the text.

[23] Some of these results can be extended to $\delta < 0$.

[24] A. Ramires and J. L. Lado, arXiv:1803.04400.

[25] G. E. Volovik, Pisma Zh. Eksp. Teor. Fiz. **107**, 537 (2018) [JETP Lett. **107**, 516 (2018)].

[26] B. Roy and V. Juricic, arXiv:1803.11190.

[27] H. Guo, X. Zhu, S. Feng, and R. T. Scalettar, Phys. Rev. B **97**, 235453 (2018).

[28] G. Baskaran, arXiv:1804.00627.

[29] B. Padhi, C. Setty, and P. W. Phillips, arXiv:1804.01101.

[30] S. Lederer, Y. Schattner, E. Berg, and S. A. Kivelson, Proc. Natl. Acad. Sci. USA **114**, 4905 (2017).

[31] S. Lederer, Y. Schattner, E. Berg, and S. A. Kivelson, Phys. Rev. Lett. **114**, 097001 (2015).

[32] T. A. Maier and D. J. Scalapino, Phys. Rev. B **90**, 174510 (2014).

[33] H.-H. Kuo, J.-H. Chu, J. C. Palmstrom, S. A. Kivelson, and I. R. Fisher, Science **352**, 958 (2016)

[34] S. Chakravarty, M. P. Gelfand, and S. Kivelson, Science **254**, 970 (1991).

[35] A. Auerbach, N. Manini, and E. Tosatti, Phys. Rev. B **49**, 12998 (1994).

[36] M. Capone, M. Fabrizio, C. Castellani, and E. Tosatti, Rev. Mod. Phys. **81**, 943 (2009).

[37] O. Gunnarsson, Rev. Mod. Phys. **69**, 575 (1997).

[38] A. Y. Ganin, Y. Takabayashi, Y. Z. Khimyak, S. Margadonna, A. Tamai, M. J. Rosseinsky, and K. Prassides, Nat. Mater. **7**, 367 (2008).

[39] Y. Takabayashi, A. Y. Ganin, P. Jeglic, D. Arcon, T. Takano, Y. Iwasa, Y. Ohishi, M. Takata, N. Takeshita, K. Prassides *et al.*, Science **323**, 1585 (2009).

[40] A. Y. Ganin, Y. Takabayashi, P. Jeglic, D. Arcon, A. Potocnik, P. J. Baker, Y. Ohishi, M. T. McDonald, M. D. Tzirakis, A. McLennan, G. R. Darling, M. Takata, M. J. Rosseinsky, and K. Prassides, Nature (London) **466**, 221 (2010).

[41] M. Granath and S. Ostlund, Phys. Rev. B **66**, 180501 (2002).

[42] M. Granath and S. Ostlund, Phys. Rev. B **68**, 205107 (2003).